

# SCIENTIFIC REPORTS



OPEN

## Skeletal muscle alkaline Pi pool is decreased in overweight-to-obese sedentary subjects and relates to mitochondrial capacity and phosphodiester content

Received: 17 August 2015  
Accepted: 16 December 2015  
Published: 03 February 2016

Ladislav Valkovič<sup>1,2,3,4</sup>, Marek Chmelík<sup>1,2</sup>, Barbara Ukropcová<sup>5,6</sup>, Thomas Heckmann<sup>7</sup>, Wolfgang Bogner<sup>1,2</sup>, Ivan Frollo<sup>3</sup>, Harald Tschan<sup>7</sup>, Michael Krebs<sup>8</sup>, Norbert Bachl<sup>7</sup>, Jozef Ukropec<sup>5</sup>, Siegfried Trattnig<sup>1,2</sup> & Martin Krššák<sup>1,2,8</sup>

Defects in skeletal muscle energy metabolism are indicative of systemic disorders such as obesity or type 2 diabetes. Phosphorus magnetic resonance spectroscopy (<sup>31</sup>P-MRS), in particular dynamic <sup>31</sup>P-MRS, provides a powerful tool for the non-invasive investigation of muscular oxidative metabolism. The increase in spectral and temporal resolution of <sup>31</sup>P-MRS at ultra high fields (i.e., 7T) uncovers new potential for previously implemented techniques, e.g., saturation transfer (ST) or highly resolved static spectra. In this study, we aimed to investigate the differences in muscle metabolism between overweight-to-obese sedentary (Ob/Sed) and lean active (L/Ac) individuals through dynamic, static, and ST <sup>31</sup>P-MRS at 7T. In addition, as the dynamic <sup>31</sup>P-MRS requires a complex setup and patient exercise, our aim was to identify an alternative technique that might provide a biomarker of oxidative metabolism. The Ob/Sed group exhibited lower mitochondrial capacity, and, in addition, static <sup>31</sup>P-MRS also revealed differences in the Pi-to-ATP exchange flux, the alkaline Pi-pool, and glycerophosphocholine concentrations between the groups. In addition to these differences, we have identified correlations between dynamically measured oxidative flux and static concentrations of the alkaline Pi-pool and glycerophosphocholine, suggesting the possibility of using high spectral resolution <sup>31</sup>P-MRS data, acquired at rest, as a marker of oxidative metabolism.

Obesity, resulting from an imbalance between energy intake and expenditure, is a worldwide epidemic associated with insulin resistance syndrome. Given that skeletal muscle accounts for almost half the total body mass and is responsible for the majority of glucose uptake and glycogen storage in response to insulin stimulus<sup>1</sup>, the investigation of muscle energy expenditure is of particular importance with regard to the pathogenesis of obesity and metabolic syndrome. Recent studies showed that insulin resistance relates to abnormalities in energy metabolism, not only of skeletal muscle<sup>2–4</sup>, but also of the heart<sup>5</sup> and liver<sup>6</sup>. The contractile activity of skeletal muscle is primarily regulated by the ATP synthesis rate<sup>7</sup>, which, under aerobic conditions in exercised muscle, is determined mainly by the oxidative phosphorylation capacity of mitochondria. Changes in muscle energy metabolism related to mitochondrial dysfunction could indicate defects in lipid metabolism (i.e., fatty acid oxidation)<sup>8</sup>, potentially

<sup>1</sup>High Field MR Centre, Department of Biomedical Imaging and Image-guided Therapy, Medical University of Vienna, Vienna, Austria. <sup>2</sup>Christian Doppler Laboratory for Clinical Molecular MR Imaging, Vienna, Austria. <sup>3</sup>Department of Imaging Methods, Institute of Measurement Science, Slovak Academy of Sciences, Bratislava, Slovakia. <sup>4</sup>Oxford Centre for Clinical MR Research (OCMR), University of Oxford, Oxford, United Kingdom. <sup>5</sup>Obesity section, Diabetes and Metabolic Disease Laboratory, Institute of Experimental Endocrinology, Slovak Academy of Sciences, Bratislava, Slovakia. <sup>6</sup>Institute of Pathophysiology, Faculty of Medicine, Comenius University, Bratislava, Slovakia. <sup>7</sup>Department of Sports and Physiological Performance, Centre of Sports Science, University of Vienna, Vienna, Austria. <sup>8</sup>Division of Endocrinology and Metabolism, Department of Internal Medicine III, Medical University of Vienna, Vienna, Austria. Correspondence and requests for materials should be addressed to M.K. (email: martin.krssak@meduniwien.ac.at)

resulting in the progression of metabolic disease, such as type 2 diabetes, even in a young, overweight-to-obese, sedentary population<sup>9–11</sup>.

The non-invasive detection of intramyocellular energy metabolites (i.e., phosphocreatine [PCr], ATP, and inorganic phosphate [Pi]) is possible through phosphorous magnetic resonance spectroscopy (<sup>31</sup>P-MRS), which provides an ideal tool for the *in vivo* monitoring of cellular energy status and metabolism<sup>7,12</sup>. Dynamic <sup>31</sup>P-MRS, during exercise and recovery, in particular, allows direct estimation of the oxidative ATP synthesis rate in challenged muscle<sup>12–15</sup>, which reflects maximal mitochondrial capacity<sup>7</sup>. Altered mitochondrial metabolism is associated with obesity, elevated fasting glucose or insulin resistance<sup>16–20</sup>. As the dynamic examinations require a complex setup, e.g., dedicated ergometers, and patient compliance throughout the whole exercise protocol, an alternative <sup>31</sup>P-MRS technique for the assessment of energy metabolism at rest would constitute a significant advantage. The measurement of resting Pi-to-ATP flux ( $F_{ATP}$ ) using <sup>31</sup>P-MRS saturation transfer (ST), correlates with the findings of dynamic experiments<sup>21,22</sup>. Although the absolute values of  $F_{ATP}$  do not provide a direct measure of oxidative metabolism<sup>23</sup>, it has also been related to insulin resistance<sup>24,25</sup>.

Recently, the use of <sup>31</sup>P-MR spectra, measured in the equilibrium state, has been promoted to obtain similar information about muscle energy metabolism. In particular, the concentration of phosphodiester ([PDE]) was shown to correlate with the Pi-to-ATP flux<sup>26</sup>. Moreover, an alkaline Pi pool ( $Pi_2$ ) has been detected *in vivo* at ultra-high field (i.e., 7T)<sup>27</sup>, and related to the PCr re-synthesis rate after exercise<sup>28</sup>.

Our aim was to compare the skeletal muscle metabolism of overweight-to-obese sedentary (Ob/Sed) subjects, who are prone to type 2 diabetes, and lean active (L/Ac) individuals, using static and dynamic <sup>31</sup>P-MRS measurements in the quadriceps femoris muscle at 7 T. In addition, the interrelations between the derived parameters were investigated to determine possible alternatives to exercise-recovery experiments.

## Results

**Between groups comparison.** In addition to a significantly higher BMI and lower  $VO_{2max}$ , the Ob/Sed individuals also differed from the L/Ac volunteers in the metabolic parameters derived from <sup>31</sup>P-MRS. The concentration of the main muscular PDE (i.e., glycerophosphocholine [GPC]), as well as the total [PDE], were significantly higher, while the concentration of the alkaline Pi-pool ( $[Pi_2]$ ) and its ratio to the main Pi concentration ( $[Pi_1]$ ), i.e., ( $Pi_2/Pi$ ), were significantly lower in the Ob/Sed group compared to the L/Ac group. In addition, the group of Ob/Sed subjects had significantly lower mitochondrial capacity ( $Q_{max}$ ) and Pi-to-ATP exchange flux ( $F_{ATP}$ ) values compared to the L/Ac group. Detailed information about the measured physiological and muscle energy metabolism parameters are listed in Table 1. In Fig. 1 are depicted representative <sup>31</sup>P-MR spectra acquired at rest and during the exercise-recovery experiment and Fig. 2 depicts the comparison between the groups.

**Correlations between the measured parameters.** The measured concentration of PDE in the quadriceps muscle correlated positively with both age ( $r = 0.45$ ,  $p = 0.014$ ) and BMI ( $r = 0.62$ ,  $p = 0.0004$ ). BMI correlated negatively with the  $[Pi_2]$  ( $r = -0.56$ ,  $p = 0.002$ ), as well as with the  $Pi_2/Pi$  ratio ( $r = -0.44$ ,  $p = 0.023$ ) and  $Q_{max}$  ( $r = -0.39$ ,  $p = 0.039$ ). The calculated  $F_{ATP}$  was also found to be negatively correlated with age ( $r = -0.48$ ,  $p = 0.009$ ) and BMI ( $r = -0.51$ ,  $p = 0.007$ ).

In addition, we have found correlations between the metabolic parameters extracted from the <sup>31</sup>P-MRS measurements performed at rest and the oxidative metabolism markers measured in a dynamic exercise-recovery experiment. The [PDE] correlated negatively with  $Q_{max}$  ( $r = -0.51$ ,  $p = 0.005$ ), while both  $[Pi_2]$  and  $Pi_2/Pi$  correlated with  $Q_{max}$  positively ( $r = 0.68$ ,  $p = 0.0001$  and  $r = 0.65$ ,  $p = 0.0002$ , respectively).  $Q_{max}$  significantly correlated also with the  $k_{ATP}$  ( $r = 0.51$ ,  $p = 0.005$ ) and  $F_{ATP}$  ( $r = 0.63$ ,  $p = 0.0003$ ). Several correlations were also found between the different parameters of muscular energy metabolism measured at rest. The [PDE] correlated negatively with  $[Pi_2]$  ( $r = -0.63$ ,  $p = 0.0003$ ),  $Pi_2/Pi$  ( $r = -0.63$ ,  $p = 0.0003$ ),  $k_{ATP}$  ( $r = -0.54$ ,  $p = 0.003$ ), and  $F_{ATP}$  ( $r = -0.59$ ,  $p = 0.001$ ). Both  $[Pi_2]$  and  $Pi_2/Pi$  were correlated with  $k_{ATP}$  ( $r = 0.41$ ,  $p = 0.029$  and  $r = 0.52$ ,  $p = 0.005$ ), as well as with  $F_{ATP}$  ( $r = 0.59$ ,  $p = 0.001$  and  $r = 0.45$ ,  $p = 0.018$ ). All correlations of the evaluated metabolic parameters with the [PDE] were also significant for the [GPC]. Representative correlations are depicted in Fig. 3.

Multivariate stepwise regression analysis of  $Q_{max}$  including physiological and metabolic parameters derived from <sup>31</sup>P-MRS data acquired at rest, identified  $[Pi_2]$  ( $r^2 = 0.46$ , adjusted  $r^2 = 0.44$ ,  $p = 0.0001$ ) as the strongest and  $F_{ATP}$  ( $r^2 = 0.54$ , adjusted  $r^2 = 0.50$ ,  $p = 0.00001$ ) as the second-strongest independent predictor of  $Q_{max}$ . Detailed results are given in Table 2.

## Discussion

In this study, we compared parameters of skeletal muscle metabolism, measured by static and dynamic <sup>31</sup>P-MRS methods, between a group of overweight-to-obese sedentary subjects, who are prone to diabetes, and a group of lean active individuals. We have found that the combination of increased BMI and sedentary lifestyle leads to significant differences in the alkaline Pi pool in skeletal muscle, as well as in other metabolic <sup>31</sup>P-MRS parameters, such as the concentration of PDE, the Pi-to-ATP metabolic flux, and mitochondrial capacity. In addition, significant correlations were found between the concentration of PDE, the alkaline  $Pi_2/Pi$  ratio, and the resting Pi-to-ATP exchange rate and flux, measured by <sup>31</sup>P-MRS techniques at rest, and the maximal mitochondrial oxidative flux, measured by an exercise-recovery experiment.

Dynamic <sup>31</sup>P-MRS provides a parameter closely related to training status, i.e., the mitochondrial capacity ( $Q_{max}$ ) of the muscle tissue<sup>15</sup>. This was also demonstrated in our study, as the  $Q_{max}$  of the overweight-to-obese sedentary subjects was significantly lower when compared to active, lean individuals. The correlation between  $Q_{max}$  and BMI found in this study can be explained by the decreased physical activity in more obese individuals, as our regression analysis showed a primary connection of  $Q_{max}$  with other parameters of muscle metabolism and not with BMI. This is in good agreement with a recent *in vitro* study, which found no differences in mitochondrial

Variable	Overweight Obese/Sedentary	Lean/Active
N (female)	14 (5) <sup>o</sup>	15 (5)
Age (years)	34.6 ± 7.1	29.3 ± 5.5
BMI (kg.m <sup>-2</sup> )	30.4 ± 2.3	23.1 ± 2.6 <sup>*</sup>
Body fat (%)	35.2 ± 7.1	18.3 ± 6.1 <sup>*</sup>
LBM (kg)	62.4 ± 10.9	63.0 ± 15.6
VO <sub>2max</sub> (mL.min <sup>-1</sup> .kg <sup>-1</sup> )	36.8 ± 5.3	45.9 ± 3.1 <sup>*</sup>
Steps per 24 hours	6052 ± 1166	11093 ± 4074 <sup>*</sup>
<b>static MRS</b>		
[PDE] (mM)	4.21 ± 1.12	2.82 ± 1.00 <sup>†</sup>
[GPC] (mM)	3.95 ± 1.04	2.47 ± 0.98 <sup>†</sup>
[GPE] (mM)	0.26 ± 0.27	0.23 ± 0.17
[Pi <sub>2</sub> ] (mM)	0.18 ± 0.07	0.28 ± 0.06 <sup>*</sup>
Pi <sub>2</sub> /Pi	0.05 ± 0.02	0.08 ± 0.02 <sup>*</sup>
pH <sub>rest</sub>	7.06 ± 0.04	7.05 ± 0.03
[ADP] <sub>rest</sub> (μM)	10.1 ± 0.9	9.8 ± 0.6
<b>ST</b>		
k <sub>ATP</sub> (s <sup>-1</sup> )	0.07 ± 0.02	0.08 ± 0.01
F <sub>ATP</sub> (mM.s <sup>-1</sup> )	0.25 ± 0.06	0.31 ± 0.04 <sup>†</sup>
k <sub>CK</sub> (s <sup>-1</sup> )	0.27 ± 0.05	0.25 ± 0.05
F <sub>CK</sub> (mM.s <sup>-1</sup> )	9.26 ± 2.36	8.66 ± 2.40
<b>Dynamic</b>		
PCr drop (% signal)	38.4 ± 19.4	40.4 ± 13.9
τ <sub>PCr</sub> (s)	40.9 ± 14.0	42.6 ± 15.8
V <sub>PCr</sub> (mM.s <sup>-1</sup> )	0.29 ± 0.10	0.32 ± 0.07
Q <sub>max</sub> (mM.s <sup>-1</sup> )	0.50 ± 0.08	0.58 ± 0.07 <sup>†</sup>
pH <sub>end exercise</sub>	6.97 ± 0.14	6.90 ± 0.16
[ADP] <sub>end exercise</sub> (μM)	47.8 ± 32.0	40.9 ± 15.5

**Table 1. Characteristics of the studied groups and results of muscle energy metabolism measurements via static <sup>31</sup>P-MRS, saturation transfer, and dynamic experiments.** Data are given as mean ± standard deviation. <sup>o</sup>For one volunteer from the overweight-to-obese sedentary group, only dynamic experiment data are available. Significant differences (unpaired t-test) between the groups are depicted as follows: <sup>†</sup>*p* < 0.01; <sup>\*</sup>*p* < 0.05.

respiratory capacity and mitochondrial content in myocellular tissue samples between lean and obese subjects with similar training status<sup>29</sup>. Similarly, a different *in vivo* study did not find any changes in mitochondrial capacity in humans after weight reduction stimulated by diet-only; however, if combined with increased physical activity, an improvement in aerobic capacity was observed<sup>30</sup>.

Significantly higher myocellular PDE levels were found in our Ob/Sed subjects when compared to the L/Ac group. This was further supported with the positive correlation found between [PDE] and BMI. This is in good agreement with the finding of a previous report by Szendroedi *et al.*<sup>26</sup> in subjects with a comparable physical activity index. A correlation of [PDE] and age was also reported, in the current study and in<sup>26,31</sup>; however, our regression analysis showed that physical activity and BMI, rather than age, primarily predict the PDE levels (data not shown). The increased spectral resolution of the 7 T MR system, used in our study, reveals that the measured [PDE] is mainly attributable to [GPC], with only a small contribution from glycerophosphoethanolamine ([GPE]), and that, in fact, it is the [GPC] that is responsible for the differences between the two groups. This separation in PDE signals was not visible in the previous study performed at 3 T<sup>26</sup>.

The ratio of alkaline Pi<sub>2</sub> to cytosolic Pi (Pi<sub>2</sub>/Pi) was lower in the Ob/Sed group in comparison to the L/Ac group. Recently, van Oorschot *et al.* reported a dependence of Pi<sub>2</sub>/Pi, measured in the vastus lateralis, on the training status, when they compared highly trained runners with normally active individuals<sup>28</sup>. The potential influence of BMI was, however, not considered in the aforementioned study. The results of our study suggest such a dependence of the Pi<sub>2</sub>/Pi ratio in skeletal muscle on BMI, as a linear correlation between BMI and Pi<sub>2</sub>/Pi was found. Nevertheless, the results of our regression analysis identified only [GPC] and Q<sub>max</sub> as the primary predictors of the Pi<sub>2</sub>/Pi (data not shown). The differences in Pi<sub>2</sub>/Pi found between the groups can be directly attributed to the changes in [Pi<sub>2</sub>], which was also significantly higher in the L/Ac group in comparison to the Ob/Sed group.

Although the mean F<sub>ATP</sub> values of our Ob/Sed group (F<sub>ATP</sub> = 0.25 ± 0.06 mM.s<sup>-1</sup>) are still above the decreased values reported previously in patients with type 2 diabetes (F<sub>ATP</sub> = 0.21 ± 0.05 mM.s<sup>-1</sup>)<sup>25</sup> the physical inactivity together with the overweight of our volunteers caused a significant reduction in the myocellular Pi-to-ATP metabolic flux, when compared to L/Ac individuals (F<sub>ATP</sub> = 0.31 ± 0.04 mM.s<sup>-1</sup>).

**Interrelations between metabolic parameters measured by dynamic and static <sup>31</sup>P-MRS.** We report several correlations between the parameters of static <sup>31</sup>P-MR spectra, exchange rates and metabolite fluxes

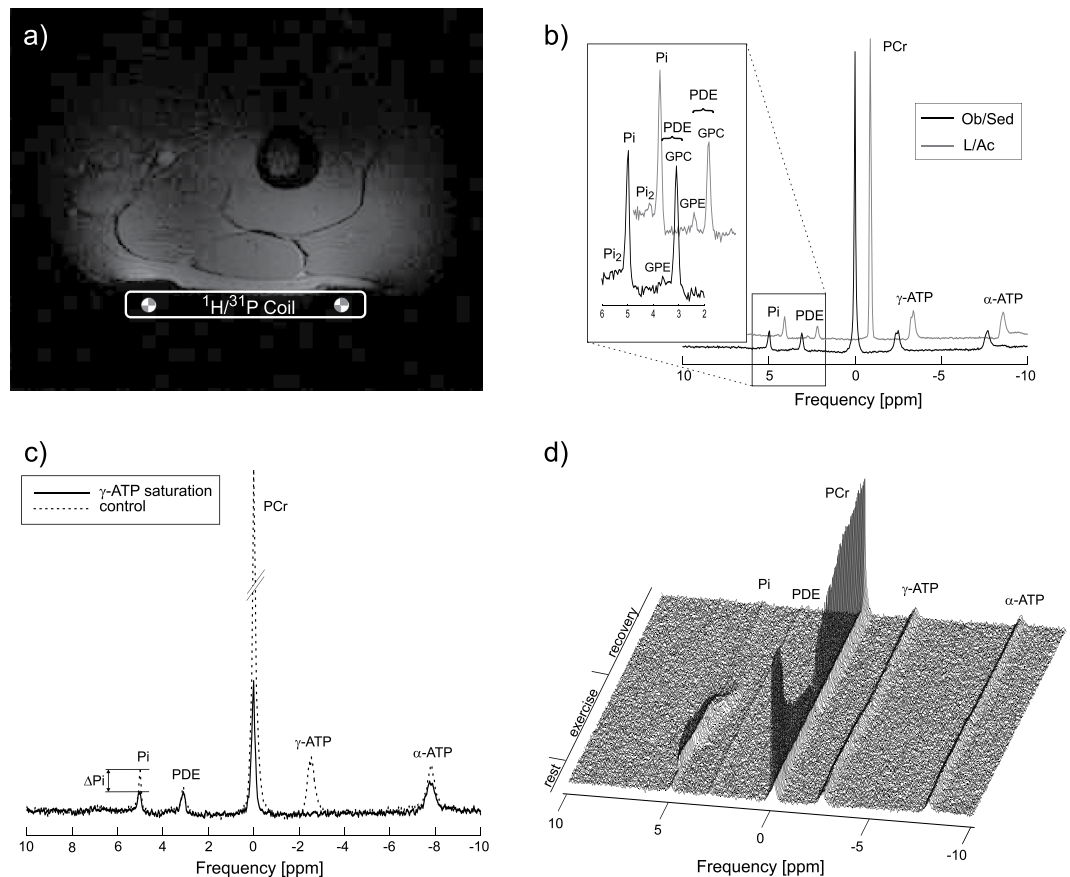


**Figure 1.** (a) An *in vivo* localizer image of the human thigh with the depicted coil position. (b) Highly spectrally resolved representative  $^{31}\text{P}$ -MR spectra from an obese sedentary and lean active subject, scaled to PCr signal intensity. The area of Pi and PDE peaks is enlarged. Note higher  $\text{Pi}_2$  and lower PDE signal intensity in the L/Ac subject. (c) Saturation transfer spectra showing the effect of  $\gamma$ -ATP saturation (solid line) on its chemical exchange partner, Pi, compared with the control experiment (dashed line). (d) Time course of the  $^{31}\text{P}$  spectra during a dynamic  $^{31}\text{P}$ -MRS experiment. Note the PCr signal depletion during exercise and its re-synthesis during recovery.

measured by ST at rest, and oxidative metabolism markers measured by exercise-recovery experiments. The alkaline  $\text{Pi}_2$  resonance is suspected to represent mitochondrial density in the muscle tissue and depends on the amount of regular physical activity<sup>28</sup>. Its relation to training status was also confirmed in our study, as the  $[\text{Pi}_2]$ , as well as  $\text{Pi}_2/\text{Pi}$ , positively correlated with the maximal oxidative flux ( $Q_{\max}$ ), determined during the dynamic experiment, and also with the  $k_{\text{ATP}}$  and  $F_{\text{ATP}}$  defining the Pi-to-ATP exchange rate and metabolic flux. Linear correlations between  $Q_{\max}$  and metabolic parameters measured by ST experiments at rest (i.e.,  $k_{\text{ATP}}$  and  $F_{\text{ATP}}$ ) reported in our previous study on overweight-to-obese subjects<sup>22</sup>, were also found in this study combining the two different population groups. In addition, the multivariate regression analysis identified  $[\text{Pi}_2]$  and  $F_{\text{ATP}}$  as independent predictors of  $Q_{\max}$ , suggesting the potential use of highly spectrally resolved static  $^{31}\text{P}$ -MRS at 7 T and ST as alternative techniques to dynamic exercise-recovery experiments.

The identified correlation between [PDE] and measured Pi-to-ATP metabolite flux ( $F_{\text{ATP}}$ ) is in good agreement with a recent report by Szendroedi *et al.*<sup>26</sup>. Significant correlations were found also between [PDE] and mitochondrial capacity ( $Q_{\max}$ ), as well as other  $^{31}\text{P}$ -MR parameters of muscle metabolism measured at rest, i.e.,  $[\text{Pi}_2]$ ,  $\text{Pi}_2/\text{Pi}$ , and  $k_{\text{ATP}}$ . In addition, the main contributors to total [PDE] were analyzed and all [PDE] correlations were also significant for [GPC]. Our results suggest the potential of using [PDE], or, if distinguishable (i.e., at 7 T) directly, the [GPC], as a surrogate biomarker of skeletal muscle energy metabolism. Although it is not perfectly clear what links GPC to muscle energy metabolism, previous studies support this finding<sup>32–37</sup>. In particular, Farber *et al.*, studying a model of membrane defect of Alzheimer's disease, reported that an inhibition of oxidative phosphorylation causes accumulation of GPC through accelerated PC turnover<sup>34</sup>. Impaired oxidative metabolism and elevated PDE levels have been also reported in patients with spinal cord injury<sup>35</sup> and congenital lipodystrophy<sup>36</sup>. Muscular PDE content was also related to glucometabolic control in type II diabetes<sup>26</sup>. Furthermore, excessive amounts of PDE have been reported in fibromyalgia<sup>33</sup>, Duchenne muscular dystrophy<sup>32</sup>, or Becker muscular dystrophy<sup>37</sup>, connecting abnormal membrane metabolism with muscle dysfunction. Nonetheless, further investigations of this relation are still necessary.

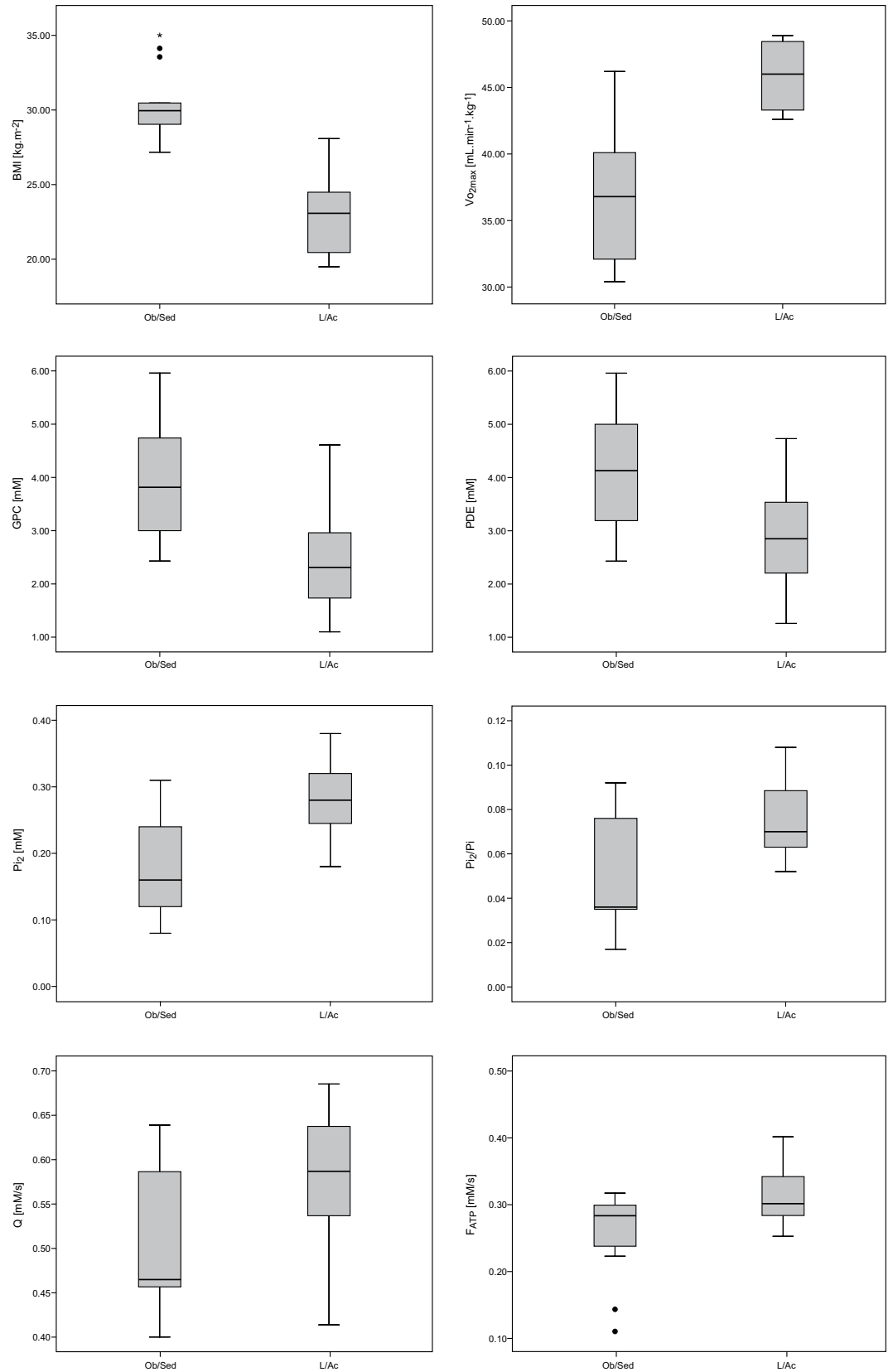


**Figure 2.** Box plots depicting the significantly different physiological and metabolic parameters between the two groups. The solid lines represent the median, boxes represent lower and upper quartiles, and whiskers the minimum and maximum. Outliers and extreme outliers are denoted by circles and stars, respectively. The outliers were also taken into account for all statistical tests.

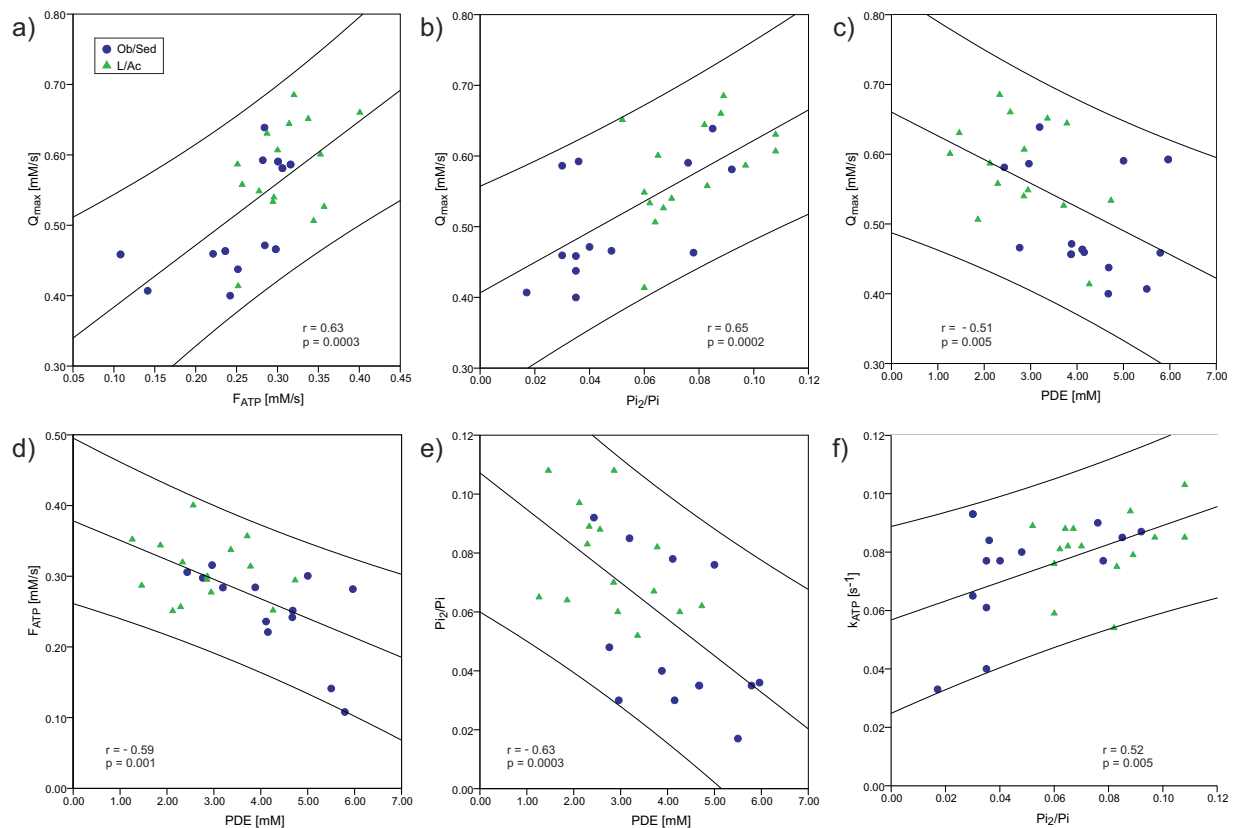


**Figure 3.** Plots of correlations between myocellular energy metabolism parameters measured by dynamic and static  $^{31}\text{P}$ -MRS in Ob/Sed (●) and L/Ac (▲) individuals: (a) mitochondrial capacity ( $Q_{\max}$ ) with the Pi-to-ATP forward metabolic flux at rest ( $F_{\text{ATP}}$ ); (b)  $Q_{\max}$  with the ratio of alkaline Pi to main Pi ( $\text{Pi}_2/\text{Pi}$ ); and (c)  $Q_{\max}$  with the concentration of phosphodiesteres ([PDE]). Further correlations of the  $^{31}\text{P}$ -MRS parameters measured at rest: (d)  $F_{\text{ATP}}$  with [PDE]; (e)  $\text{Pi}_2/\text{Pi}$  with [PDE]; and (f) Pi-to-ATP exchange rate constant ( $k_{\text{ATP}}$ ) with  $\text{Pi}_2/\text{Pi}$ . 95% confidence intervals are also depicted.

Independent variables per $Q_{\max}$	F value	p value
$\text{Pi}_2^*$	22.035	0.0001
$F_{\text{ATP}}^*$	14.653	0.0001
$\text{Pi}_2/\text{Pi}$	<0.05	0.217
BMI	<0.05	0.536
$k_{\text{ATP}}$	<0.05	0.537
GPC	<0.05	0.689
PDE	<0.05	0.940
age	<0.05	0.961

**Table 2.** Results of multivariable stepwise regression of  $Q_{\max}$  (dependent variable) and physiological and metabolic variables measured at rest (independent variable). \*Variables accepted into the model as predictors; all other variables not accepted into the model.

The findings of this study support our previous report on correlations between dynamic and ST parameters in this Ob/Sed group<sup>22</sup> and provide additional information through analysis of  $\text{Pi}_2/\text{Pi}$  and GPC, and moreover, by comparison to a lean active group of individuals. As to the technical limitations of our study, we should note that although care was taken to perfectly reposition the subject in the second MR system, when applicable, some small mislocalizations could not be fully excluded. The effect of individual anatomy must be also considered, as the localization through the sensitivity of the surface coil used in this study might cover different portions of the quadriceps muscles between subjects. Localization techniques, recently proposed for dynamic examinations of the lower leg muscles, e.g., frequency selective  $^{31}\text{P}$ -MRI<sup>38–40</sup>, semi-LASER for single voxel localization<sup>41</sup> or depth-resolved surface coil MRS<sup>42</sup>, could be used in future studies to measure muscle-specific metabolism. However, the muscles of the quadriceps covered by the sensitivity volume of the used surface coil are all active

during knee-extension<sup>43</sup>, and, therefore, the inter-subject variability of the covered muscle volumes should have had only a minor effect on our results.

In conclusion, overweight-to-obese sedentary pre-diabetics exhibit increased concentrations of glycerophosphocholine, a lower amount of alkaline Pi, a slower Pi-to-ATP exchange rate, and decreased mitochondrial capacity compared to lean active individuals. Associations found between the parameters of mitochondrial metabolism measured at rest and during exercise suggest that highly spectrally resolved static <sup>31</sup>P-MRS and saturation transfer measurements at rest could provide markers of muscle mitochondrial metabolism.

## Methods

Fifteen young, overweight-to-obese, sedentary individuals (10/5 male/female; age  $34.6 \pm 7.1$  years) with a body mass index (BMI)  $\geq 27.0$  kg.m<sup>-2</sup>, a sedentary lifestyle without regular physical activity, no pharmacotherapy, and no medical history of type 2 diabetes were recruited for this study and classified as the overweight-to-obese/sedentary (Ob/Sed) group. Thirteen of these volunteers had already participated in our previous study on the interrelations between mitochondrial capacity and Pi-to-ATP exchange rates in this particular type of population<sup>22</sup>. Fifteen young, lean, physically active participants (10/5 male/female; age  $29.3 \pm 5.5$  years) were recruited for the current study as the control lean/active (L/Ac) group.

Written, informed consent was obtained from each participant in the study after an explanation of the purpose, nature and potential risks of the study. The examination protocol was approved by the appropriate institutional ethical boards of the Medical University of Vienna and of the University Hospital Bratislava, Comenius University Bratislava, and the study was carried out in accordance with the approved guidelines.

**Physiological tests.** Within a week before the MR examination, the participants underwent a physical examination and physiological testing. BMI was measured by an analog weight scale and standard measuring tape. Bioelectric impedance, measured using an Omron BF511 (Omron Healthcare, Matsusaka, Japan), was used to evaluate total adiposity (%Fat) and to estimate the lean body mass (LBM). The maximal aerobic capacity (i.e., whole-body oxygen uptake [VO<sub>2max</sub>]) was measured during an incremental exercise test performed on a Lode Corival cycle ergometer (Lode, Groningen, The Netherlands). Continuous measurement of the gas exchange rate was obtained with the Ergostik (Geratherm Respiratory, Bad Kissingen, Germany), and the maximal oxygen consumption rate was expressed relative to LBM. The ergometry was performed at least three days prior to the MR examinations. The activity level was evaluated based on two working days and a weekend of accelerometer recordings and expressed as the number of steps per 24 hours.

**<sup>31</sup>P-MRS.** Each participant underwent the entire MR examination protocol in one day, starting two hours after a standardized meal. The dynamic <sup>31</sup>P-MRS exercise-recovery experiment was performed on either a 7 T MR system (Magnetom, Siemens Healthcare, Erlangen, Germany) or a 3 T MR system (TIM Trio) from the same manufacturer, due to initial compatibility problems of our ergometer (Quadspect, Ergospect, Innsbruck, Austria) with the 7 T. Dual-tuned (<sup>31</sup>P-<sup>1</sup>H) circular surface coils (10 cm diameter, Rapid Biomedical, Rimpar, Germany), with similar sensitivity volumes<sup>22</sup> were used on both MR systems. The use of two MR systems, equipped with the same ergometer and surface coils with a similar sensitivity volume, has recently been shown to have no effect on the metabolic data derived from dynamic <sup>31</sup>P-MRS<sup>44</sup>.

Static <sup>31</sup>P-MRS experiments were performed exclusively at 7 T, as the increased spectral resolution is necessary for separation of the Pi<sub>2</sub>, as well as the GPE and GPC signals<sup>27</sup>, and the increase in signal-to-noise ratio allows significant reduction in measurement time of the ST experiment, compared to 3 T<sup>45</sup>. The subjects were investigated while lying inside the MR scanner with the surface coil fixed to the quadriceps femoris muscle (Fig. 1a) and the coil positions were marked to allow precise repositioning in the other MR system, if applicable. When the dynamic measurements were performed at 3 T (i.e., in case of first 10 Ob/Sed subjects), the order of examinations was randomized to allow simultaneous examinations of two subjects; otherwise the measurements at rest were always performed prior to the exercise-recovery experiment.

For the assessment of intramyocellular metabolite concentrations and the Pi<sub>2</sub>/Pi ratio, a pulse-acquire <sup>31</sup>P-MR spectrum (acquisition delay = 0.4 ms; repetition time = 15 s; bandwidth = 5 kHz; 16 averages in 4 minutes) was acquired at rest (Fig. 1b) and corrected for longitudinal relaxation times, as measured for <sup>31</sup>P muscle metabolites at 7 T<sup>27,46</sup>. The  $\gamma$ -ATP signal was used as an internal concentration reference, assuming a stable ATP concentration of 8.2 mM in the skeletal muscle<sup>12</sup>.

The exchange rate between ATP and Pi (i.e., ATP synthesis) was investigated using an ST experiment applying continuous irradiation, and the apparent longitudinal relaxation time (T<sub>1</sub><sup>app</sup>) was determined via an inversion recovery experiment, as described previously<sup>45</sup>. The total measurement time of the ST experiment was under 9 minutes.

The exercise-recovery protocol involved six minutes of repeated knee extensions against an air pressure, set to 30% of the maximal voluntary contraction force, once every repetition time (i.e., 2 s), followed by six minutes of recovery<sup>15</sup>. The volunteers were instructed by an audio signal to time the contraction-relaxation periods, so that the spectra were acquired always in the relaxed state of the muscle.

**Analyses and calculations.** Due to patient noncompliance (n<sub>Ob/Sed</sub> = 1) and technical problems (n<sub>Ob/Sed</sub> = 1), 28 complete datasets and one incomplete dataset (dynamic <sup>31</sup>P-MRS only), were available for analyses.

All acquired <sup>31</sup>P-MR spectra were analyzed using jMRUI software with the AMARES time domain fitting algorithm<sup>47</sup>. The resonance lines of PCr, two Pi signals, and two PDEs—glycerophosphocholine (GPC) and glycerophosphoethanolamine (GPE)—were fitted as single Lorentzians, whereas  $\gamma$ - and  $\alpha$ -ATP were fitted as doublets and  $\beta$ -ATP as a triplet. The line width of the Pi<sub>2</sub> peak was constrained with respect to the line width of the main Pi peak, and the expected frequency difference between Pi<sub>2</sub> and Pi was set to ~0.4 ppm, to ensure a good

fit for the  $Pi_2$  peak<sup>27,28</sup>. The shift in resonance position between PCr and Pi signals in parts per million ( $\delta$ ) was used to calculate intramyocellular pH<sup>48</sup>, according to the Henderson-Hasselbalch equation:  $pH = 6.75 + \log((\delta - 3.27)/(5.63 - \delta))$ . The free cytosolic ADP concentration ([ADP]) was calculated according to the method described by Kemp *et al.*<sup>49</sup>, assuming that 15% of total creatine [Cr] was not phosphorylated in the resting state<sup>50</sup>.

The chemical exchange rate constant ( $k_{ATP}$ ) was calculated from the fractional reduction of Pi magnetization upon selective saturation of  $\gamma$ -ATP (Fig. 1c)<sup>45</sup>. The resting unidirectional forward exchange flux was then calculated as  $F_{ATP} = k_{ATP} \times [Pi]$ .

To calculate the time constant of PCr resynthesis ( $\tau_{PCr}$ ), the PCr signal changes during the recovery period of the dynamic experiment (Fig. 1d) were fitted to a monoexponential function using MATLAB (MathWorks, Natick, MA, USA). The initial PCr recovery rate ( $V_{PCr}$ ), which roughly represents ATP turnover at the end of exercise, was determined and used to calculate the maximal rate of oxidative phosphorylation ( $Q_{max}$ ) according to the ADP-based model of Michaelis and Menten<sup>49</sup>.

Data are presented as means  $\pm$  standard deviations and compared between the groups by an unpaired Student t-test. The relationships between metabolic parameters were analyzed by linear regression analysis, using Pearson's correlation coefficient, to estimate the strength of the relationship. Multivariate stepwise regression analysis for the dependent variable  $Q_{max}$  was performed using the independent variables (i.e., BMI, age, [PDE], [GPC],  $[Pi_2]$ ,  $Pi_2/Pi$ ,  $k_{ATP}$ , and  $F_{ATP}$ ). A similar multivariate regression analysis was performed for the dependent variables [PDE] and  $Pi_2/Pi$ . The results were considered statistically significant at  $p < 0.05$ .

**Data.** Parts of the data were presented as abstracts at the following meetings: ISMRM 2012 Melbourne Australia, ISMRM 2015 Toronto Canada. Some <sup>31</sup>P-MRS data of the dynamic and ST experiment, from the Ob/Sed group exclusively, were published in the *NMR in Biomedicine* journal (ref. 22).

## References

- DeFronzo, R. A., Bonadonna, R. C. & Ferrannini, E. Pathogenesis of NIDDM. A balanced overview. *Diabetes Care*. **15**, 318–368 (1992).
- Kelley, D. E., He, J., Menshikova, E. V. & Ritov, V. B. Dysfunction of mitochondria in human skeletal muscle in type 2 diabetes. *Diabetes*. **51**, 2944–2950 (2002).
- Rabol, R., Boushel, R. & Dela, F. Mitochondrial oxidative function and type 2 diabetes. *Appl Physiol Nutr Metab*. **31**, 675–683 (2006).
- Little, J. P. *et al.* Low-volume high-intensity interval training reduces hyperglycemia and increases muscle mitochondrial capacity in patients with type 2 diabetes. *J Appl Physiol* (1985). **111**, 1554–1560 (2011).
- Perseghin, G. *et al.* Abnormal left ventricular energy metabolism in obese men with preserved systolic and diastolic functions is associated with insulin resistance. *Diabetes Care*. **30**, 1520–1526 (2007).
- Schmid, A. I. *et al.* Liver ATP synthesis is lower and relates to insulin sensitivity in patients with type 2 diabetes. *Diabetes Care*. **34**, 448–453 (2011).
- Kemp, G. J. & Radda, G. K. Quantitative interpretation of bioenergetic data from <sup>31</sup>P and <sup>1</sup>H magnetic resonance spectroscopic studies of skeletal muscle: an analytical review. *Magn Reson Q*. **10**, 43–63 (1994).
- Hood, D. A. Invited Review: contractile activity-induced mitochondrial biogenesis in skeletal muscle. *J Appl Physiol* (1985). **90**, 1137–1157 (2001).
- Morino, K., Petersen, K. F. & Shulman, G. I. Molecular mechanisms of insulin resistance in humans and their potential links with mitochondrial dysfunction. *Diabetes*. **55** Suppl 2, S9–S15 (2006).
- Ukropec, J. *et al.* Adipose tissue and skeletal muscle plasticity modulates metabolic health. *Arch Physiol Biochem*. **114**, 357–368 (2008).
- Wells, G. D. *et al.* Skeletal muscle metabolic dysfunction in obesity and metabolic syndrome. *Can J Neurol Sci*. **35**, 31–40 (2008).
- Kemp, G. J., Meyerspeer, M. & Moser, E. Absolute quantification of phosphorus metabolite concentrations in human muscle *in vivo* by <sup>31</sup>P MRS: a quantitative review. *NMR Biomed*. **20**, 555–565 (2007).
- Quistorff, B., Johansen, L. & Sahlin, K. Absence of phosphocreatine resynthesis in human calf muscle during ischaemic recovery. *Biochem J*. **291** (Pt 3), 681–686 (1993).
- Tonson, A. *et al.* Muscle energetics changes throughout maturation: a quantitative <sup>31</sup>P-MRS analysis. *J Appl Physiol* (1985). **109**, 1769–1778 (2010).
- Layec, G. *et al.* Comparative determination of energy production rates and mitochondrial function using different <sup>31</sup>P MRS quantitative methods in sedentary and trained subjects. *NMR Biomed*. **24**, 425–438 (2011).
- Newcomer, B. R., Larson-Meyer, D. E., Hunter, G. R. & Weinsier, R. L. Skeletal muscle metabolism in overweight and post-overweight women: an isometric exercise study using (<sup>31</sup>)P magnetic resonance spectroscopy. *Int J Obes Relat Metab Disord*. **25**, 1309–1315 (2001).
- Scheuermann-Freestone, M. *et al.* Abnormal cardiac and skeletal muscle energy metabolism in patients with type 2 diabetes. *Circulation*. **107**, 3040–3046 (2003).
- Schrauwen-Hinderling, V. B. *et al.* Impaired *in vivo* mitochondrial function but similar intramyocellular lipid content in patients with type 2 diabetes mellitus and BMI-matched control subjects. *Diabetologia*. **50**, 113–120 (2007).
- Perry, C. G., Kane, D. A., Lanza, I. R. & Neuffer, P. D. Methods for assessing mitochondrial function in diabetes. *Diabetes*. **62**, 1041–1053 (2013).
- Faraut, B. *et al.* Capsiate administration results in an uncoupling protein-3 downregulation, an enhanced muscle oxidative capacity and a decreased abdominal fat content *in vivo*. *Int J Obes (Lond)*. **33**, 1348–1355 (2009).
- Schmid, A. I. *et al.* Comparison of measuring energy metabolism by different (<sup>31</sup>)P-magnetic resonance spectroscopy techniques in resting, ischemic, and exercising muscle. *Magn Reson Med*. **67**, 898–905 (2012).
- Valković, L. *et al.* Interrelation of <sup>31</sup>P-MRS metabolism measurements in resting and exercised quadriceps muscle of overweight-to-obese sedentary individuals. *NMR Biomed*. **26**, 1714–1722 (2013).
- Kemp, G. J. & Brindle, K. M. What do magnetic resonance-based measurements of  $Pi \rightarrow ATP$  flux tell us about skeletal muscle metabolism? *Diabetes*. **61**, 1927–1934 (2012).
- Petersen, K. F. *et al.* Impaired mitochondrial activity in the insulin-resistant offspring of patients with type 2 diabetes. *N Engl J Med*. **350**, 664–671 (2004).
- Szendroedi, J. *et al.* Muscle mitochondrial ATP synthesis and glucose transport/phosphorylation in type 2 diabetes. *PLoS Med*. **4**, e154 (2007).
- Szendroedi, J. *et al.* Skeletal muscle phosphodiester content relates to body mass and glycemic control. *PLoS One*. **6**, e21846 (2011).
- Kan, H. E. *et al.* *In vivo* <sup>31</sup>P MRS detection of an alkaline inorganic phosphate pool with short T1 in human resting skeletal muscle. *NMR Biomed*. **23**, 995–1000 (2010).



28. van Oorschot, J. W. *et al.* 31P MR spectroscopy and computational modeling identify a direct relation between Pi content of an alkaline compartment in resting muscle and phosphocreatine resynthesis kinetics in active muscle in humans. *PLoS One*. **8**, e76628 (2013).
29. Fisher-Wellman, K. H. *et al.* Mitochondrial respiratory capacity and content are normal in young insulin-resistant obese humans. *Diabetes*. **63**, 132–141 (2014).
30. Toledo, F. G. *et al.* Mitochondrial capacity in skeletal muscle is not stimulated by weight loss despite increases in insulin action and decreases in intramyocellular lipid content. *Diabetes*. **57**, 987–994 (2008).
31. Satrustegui, J. *et al.* An *in vivo* phosphorus nuclear magnetic resonance study of the variations with age in the phosphodiester content of human muscle. *Mech Ageing Dev.* **42**, 105–114 (1988).
32. Younkin, D. P. *et al.* 31P NMR studies in Duchenne muscular dystrophy: age-related metabolic changes. *Neurology*. **37**, 165–9 (1987).
33. Park, J. H. *et al.* Use of P-31 magnetic resonance spectroscopy to detect metabolic abnormalities in muscles of patients with fibromyalgia. *Arthritis Rheum.* **41**, 406–13 (1998).
34. Farber, S. A., Slack, B. E. & Blusztajn, J. K. Acceleration of phosphatidylcholine synthesis and breakdown by inhibitors of mitochondrial function in neuronal cells: a model of the membrane defect of Alzheimer's disease. *FASEB J.* **14**, 2198–206 (2000).
35. McCully, K. K., Mulcahy, T. K., Ryan, T. E. & Zhao, Q. Skeletal muscle metabolism in individuals with spinal cord injury. *J Appl Physiol* (1985). **111**, 143–8 (2011).
36. Sleight, A. *et al.* Mitochondrial oxidative phosphorylation is impaired in patients with congenital lipodystrophy. *J Clin Endocrinol Metab.* **97**, E438–42 (2012).
37. Wokke, B. H. *et al.* Muscle MRS detects elevated PDE/ATP ratios prior to fatty infiltration in Becker muscular dystrophy. *NMR Biomed.* **27**, 1371–7 (2014).
38. Parasoglou, P., Xia, D., Chang, G. & Regatte, R. R. Dynamic three-dimensional imaging of phosphocreatine recovery kinetics in the human lower leg muscles at 3T and 7T: a preliminary study. *NMR Biomed.* **26**, 348–356 (2013).
39. Parasoglou, P., Xia, D., Chang, G. & Regatte, R. R. Three-dimensional saturation transfer (31)P-MRI in muscles of the lower leg at 3.0 T. *Sci Rep.* **4**, 5219 (2014).
40. Schmid, A. I. *et al.* Dynamic PCr and pH imaging of human calf muscles during exercise and recovery using (31)P gradient-Echo MRI at 7 Tesla. *Magn Reson Med.* (2015).
41. Fiedler, G. B. *et al.* Localized semi-LASER dynamic (31)P magnetic resonance spectroscopy of the soleus during and following exercise at 7 T. *MAGMA.* **28**, 493–501 (2015).
42. Valkovič, L. *et al.* Depth-resolved surface coil MRS (DRESS)-localized dynamic (31)P-MRS of the exercising human gastrocnemius muscle at 7 T. *NMR Biomed.* **27**, 1346–1352 (2014).
43. Richardson, R. S., Frank, L. R. & Haseler, L. J. Dynamic knee-extensor and cycle exercise: functional MRI of muscular activity. *Int J Sports Med.* **19**, 182–187 (1998).
44. Šedivý, P. *et al.* Dynamic 31P MR spectroscopy of plantar flexion: Influence of ergometer design, magnetic field strength (3 and 7 T), and RF-coil design. *Med Phys.* **42**, 1678–1689 (2015).
45. Valkovič, L. *et al.* Time-resolved phosphorous magnetization transfer of the human calf muscle at 3 T and 7 T: a feasibility study. *Eur J Radiol.* **82**, 745–751 (2013).
46. Bogner, W. *et al.* Assessment of (31)P relaxation times in the human calf muscle: a comparison between 3 T and 7 T *in vivo*. *Magn Reson Med.* **62**, 574–582 (2009).
47. Vanhamme, L., van den Boogaart, A. & Van Huffel, S. Improved method for accurate and efficient quantification of MRS data with use of prior knowledge. *J Magn Reson.* **129**, 35–43 (1997).
48. Moon, R. B. & Richards, J. H. Determination of intracellular pH by 31P magnetic resonance. *J Biol Chem.* **248**, 7276–7278 (1973).
49. Kemp, G. J. *et al.* Quantitative analysis by 31P magnetic resonance spectroscopy of abnormal mitochondrial oxidation in skeletal muscle during recovery from exercise. *NMR Biomed.* **6**, 302–310 (1993).
50. Boska, M. ATP production rates as a function of force level in the human gastrocnemius/soleus using 31P MRS. *Magn Reson Med.* **32**, 1–10 (1994).

## Acknowledgements

This work was supported by the Christian Doppler Society–Clinical Molecular MR Imaging (MOLIMA to S.T.), by the OeNB Jubilaefonds (grant #15363 to M.Krš., #15455 to L.V. and #16133 to W.B.), by the AKTION Austria–Slovak Republic (grant #2013-10-15-004), by an EFSD & Lilly research fellowship to B.U., by the Slovak Grant Agency (VEGA grants #2/0013/14, #2/0192/14 and APVV grant #0431-12), and by a Sir Henry Dale Fellowship from the Wellcome Trust and the Royal Society [098436/Z/12/Z].

## Author Contributions

L.V., B.U., J.U. and M.K. designed the study, L.V., M.C. and T.H. acquired and analyzed the data. L.V. and M.K. wrote the manuscript. W.B., I.F., H.T., M.K., N.B., J.U. and S.T. contributed to the discussion and all authors reviewed the final form of the manuscript.

## Additional Information

**Competing financial interests:** The authors declare no competing financial interests.

**How to cite this article:** Valkovič, L. *et al.* Skeletal muscle alkaline Pi pool is decreased in overweight-to-obese sedentary subjects and relates to mitochondrial capacity and phosphodiester content. *Sci. Rep.* **6**, 20087; doi: 10.1038/srep20087 (2016).



This work is licensed under a Creative Commons Attribution 4.0 International License. The images or other third party material in this article are included in the article's Creative Commons license, unless indicated otherwise in the credit line; if the material is not included under the Creative Commons license, users will need to obtain permission from the license holder to reproduce the material. To view a copy of this license, visit <http://creativecommons.org/licenses/by/4.0/>